Available online at www.sciencedirect.com
ScienceDirect
Journal of the European Ceramic Society 27 (2007) 4181–4186
www.elsevier.com/locate/jeurceramsoc

Hydroxyapatite nanoceramics: Basic physical properties and biointerface modification

Daniel Aronov [a], Anatoly Karlov [b], Gil Rosenman [a,*]

[a] School of Electrical Engineering, Department of Physical Electronics, Tel-Aviv University, 69978 Ramat-Aviv, Israel
[b] Center for Orthopedic and Medical Material Sciences of the Siberian Branch of the Russian Academy of Medical Sciences, 634029 Tomsk, Russia

Available online 9 April 2007

Abstract

A new method of surface energy modification and engineering of the hydroxyapatite (HAp) nanoceramics coatings is presented. It is performed by electron-induced surface energy modification resulting in deep and tunable variation of its wettability state. It is found from electronic traps state spectroscopy studies of the HAp ceramics implemented by various methods such as photoluminescence and surface photovoltage spectroscopy, that the HAp nanoceramics is a wide band gap p-type semiconductor with complex structure of electron/hole bulk and surface localized states. It is shown that a low-energy electron irradiation leads to surface potential modulation and provides tailoring any wettability state in a wide range of contact angles by variation of injected and trapped electron charge. The diverse wettability states engineered on the HAp surface enable selective adhesion of basic biological cells such as proteins, DNA and various bacteria.

Keywords: Apatite; Nanocomposite; Surfaces; Interfaces; Biomedical application

1. Introduction

The promising trends in biotechnology and tissue engineering are based on development of advanced materials with biomimetic features created by designing and tailoring of specific surface properties.[1] The modification of surface properties is directed to enhance the surface affinity to selective adhesion and proliferation of biological cells, improvement of biological response, and tissue compatibility.[2]

Among various biocompatible materials, hydroxyapatite (HAp) is widely used in many biomedical applications. HAp is natural mineral ingredient of bones, tooth and calcified tissues in vertebrate. Man-made HAp is served for human implant coatings possessing beneficial biocompatibility and osteoconductivity resulting in bonding to a human hard tissue. It is known as a substrate for effective adhesion of proteins, peptides, lipids, bacteria, and strains.[3,4]

In this work, we present a new approach to interface engineering of the HAp nanoceramics coatings performed by electron-induced surface energy modification resulting in deep and tunable variation of its wettability (hydrophobic/hydrophilic) state.[5] It is found from studies of electronic traps state spectroscopy of the HAp that the HAp nanoceramics is a wide band gap p-type semiconductor with complex structure of electron/hole bulk and surface localized states. It is shown that a low-energy electron irradiation leads to surface potential modulation and provides tailoring any wettability state in a wide range of contact angles by variation of injected and trapped electron charge. The diverse wettability states engineered on the HAp surface enable selective adhesion of basic biological cells such as proteins, DNA and various bacteria.

2. Material surface modification and biocompatibility

The key problem in biomedical and surface science is based on development of smart substrates with modified interface for amplifying affinity to biomolecules adhesion and biocells immobilization.[1–4] Several diverse techniques have been developed for adapting biological substrates with interacted cells including deposition of self-assembled monolayers, electrical, light-induced and electrochemical methods, *etc*.[1,2] The common feature of the applied techniques is modification of the original surface energy and related properties (wettability, adsorption, adhesion, *etc*.) of the substrates. However, these methods are accompanied by surface chemical reactions, phase transitions,

* Corresponding author.
E-mail address: gilr@eng.tau.ac.il (G. Rosenman).

0955-2219/$ – see front matter © 2007 Elsevier Ltd. All rights reserved.
doi:10.1016/j.jeurceramsoc.2007.02.121

defects' creation or foreign molecules structure formation on the modified surfaces.

Analyses of numerous publications show that there is no a commonly accepted microscopic mechanism of biocells adhesion.[1] Among various types of adsorptive mechanisms van der Waals, hydrogen-bonding, electrostatic, lectin-like, and hydrophobic–hydrophilic interactions have been considered as a basis for effective adhesion of cells at a substrate.[1,2] A wide basic research has shown that the wettability modification may strongly affect biocompatibility of materials.[1,6] In particular, the origin of adhesion in HAp-based orthopedic implants for some biocells and microorganisms such as proteins[6] and bacteria[1] is mainly ascribed to wettability of the substrates, considering wettability properties as a leading mechanism that responsible for biocells immobilization. However, the methods applied to modify surface energy and wettability properties of biosubstrates mainly allow on/off switching of the wettability.[1]

Another approach, which is applied to modify the HAp surface adhesion affinity to biological cells, is electron irradiation of the HAp ceramics or coatings followed by the charge trapping on the surface states and bulk states localized in the vicinity of the surface.[5]

3. Hydroxyapatite physical properties and electronic structure

In this work the HAp particles of typical 40 nm size were extracted from nanopowder mass and used as a raw material for preparation of the ceramic samples.[7] The platelet-like samples (height of 2 mm; diameter of 5 mm) were fabricated using dry pressing HAp powders. The X-ray diffractometry (XRD) analysis and Fourier transform infrared spectroscopy spectra of the synthesized samples showed the good formed crystalline structure of the HAp. A typical formula of the HAp is $Ca_{10-x}(HPO_4)_x(PO_4)_{6-x}(OH)_{2-x}$, where x ranges from 0 to 2, giving a Ca/P atomic ratio between 1.33 ($x = 2$) and 1.67 ($x = 0$).[8] The composition and atomic concentrations of the elements contained in the investigated HAp ceramics were determined from X-ray photoelectron spectroscopy (XPS) (5600 multi-technique system, PHI, USA) measurements. The Ca/P and O/Ca molar ratios obtained from atomic concentration measurements was found to be 1.66 and 2.78, respectively, which is the evidence that the fabricated HAp ceramics is close to the stoichiometric composition.

Topography features were studied by atomic force microscopy (AFM) (Multimode, Digital Instruments) in tapping mode. Statistical analysis of the AFM measurements gave the average size of the ceramic grains around 1.0 μm with dispersion of 0.3 μm. The fabricated samples were also characterized by porosity and root mean square roughness around 10% and 0.16 μm, respectively.

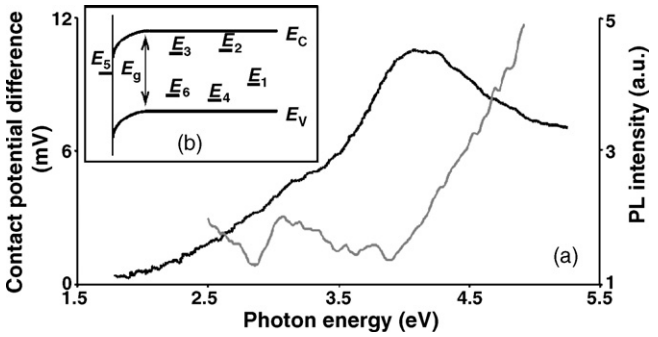

Fig. 1. (a) Surface photovoltage spectrum (black line) and photoluminescence (PL) excitation spectrum (gray line) of the hydroxyapatite ceramic sample. (b) Band diagram of the hydroxyapatite ceramic. Here E_1–E_4 and E_6 are the bulk states, E_5 are the surface state and E_g is the band gap energy. E_V and E_C refer to valence and conduction band, respectively.

We applied diverse optical methods such as photoluminescence (PL) and surface photovoltage spectroscopy (SPS) for studies of fine electron/hole trap spectrum of the HAp.[9] The experimental data (Fig. 1a, Table 1) allowed to obtain a value of the energy band gap $E_g = 3.9$ eV. Several individual energy states were also found. They are located in the energy gap in the range 2.6–3.9 eV. Comparison between the SPS and the PL spectra (Fig. 1a, Table 1) indicates that the energy spectra of electron/hole levels studied by two different experimental spectroscopy techniques are very similar (Table 1). However the electron state $E_5 = 3.3$ eV found by the SPS method was not observed in the PL spectrum. The contact potential difference, generated between the Kelvin probe and illuminated sample's surface, affected both by the surface and near surface-bulk states. However, the PL intensity totally depends on the number of states participating in recombination process resulting in photon emission. The PL is mainly contributed by the bulk states. It allows relating the electron state E_5 to the surface state, which does not contribute sufficiently to the PL. Fig. 1b demonstrates found energy structure of the studied HAp ceramics.

4. Charge-induced wettability effect and wettability modification of hydroxyapatite

Surface wettability (hydrophobicity) is a measure of the surface energy[10] and is most commonly quantified by a contact angle θ. The drop's shape is governed by the action of forces pulling at the contact line of the drop in the plane of the solid, where the solid/liquid, liquid/vapor and solid/vapor interfaces

Table 1
Energy positions of electron/(hole) states in the hydroxyapatite obtained from photoluminescence excitation (PL) and surface photovoltage spectroscopy (SPS) spectra

Method	E_1 [eV]	E_2 [eV]	E_3 [eV]	E_4 [eV]	E_5 [eV]	E_6 [eV]	E_g [eV]
PL	2.6	2.8	3.0	3.2	–	3.4	4.0
SPS	$E_C - 2.6$	$E_V + 2.9$	$E_V + 3.0$	$E_C - 3.2$	$E_V + 3.3$	$E_C - 3.4$	3.9

E_V and E_C refer to valence and conduction band, respectively.

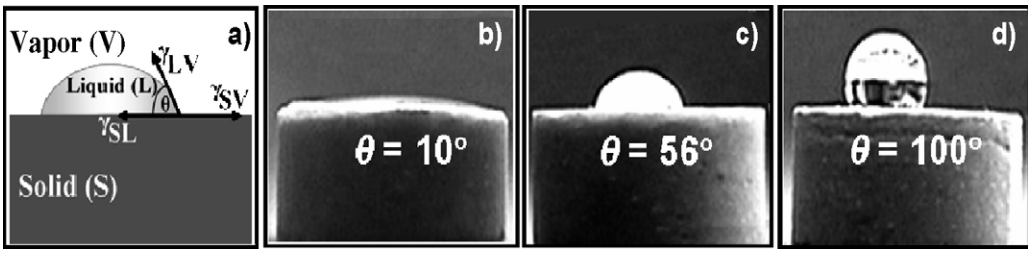

Fig. 2. (a) Schematic illustration of the wettability effect. The droplet shape is characterized by the contact angle, θ, which is defined by three interfacial energies γ_{SV} (surface/vapor), γ_{SL} (surface/liquid), and γ_{LV} (liquid/vapor). (b–d) Variation of the deionized water contact angle on the modified hydroxyapatite surface, induced by a low-energy electron irradiation: (b) initial condition, (c and d) after the electron irradiation at charge density $Q = 130$ and $300\ \mu C/cm^2$, respectively. The electron irradiation energy is $E_e = 100$ eV.

meet (Fig. 2a). Three phases are indicated by the subscripts: S is the solid; L is the liquid; and V is the corresponding equilibrium vapor. The contact angle is defined by equilibrium state between these forces acting on the contact line separating wetted and non-wetted portions of a homogenous smooth solid surface. Each interface is described by a certain free energy per unit area γ_{SL}, γ_{LV}, and γ_{SV} resulting in the Young's equation:[10] $\cos(\theta) = (\gamma_{SV} - \gamma_{SL})/\gamma_{LV}$.

It is well known that electric charge plays a significant role in the wetting phenomenon. The effect, referred as electrocapillarity—the basis of modern electrowetting and microfluidics, was first described in details in 1875 by Lippmann.[11] The charges and dipoles redistribute, modifying the surface energy at the interface liquid drop/substrate, when an external electric potential is applied between a liquid drop and solid. As a result, a sufficient enhance of the wetting is observed. It is described by modified Young's equation, when the presence of a net electric charge at an interface lowers γ_{SL}. Note that interfacial energies related to γ_{SV} and γ_{LV} remain constant and independent on the applied potential.

Recently, we found the opposite phenomenon—a decrease in the wetting.[5,12] The main difference from the conventional electrowetting effect is that the electric field is generated by a low-energy electron irradiation and affects both the solid/vapor and solid/liquid interphases, when reduction of the latter is always higher. The difference between energies, $\Delta\gamma_{SV}$ and $\Delta\gamma_{SL}$, is caused only by the disparity between the potentials, created by identical charges near various interphases. However, the corresponding potentials differ because of the various contributions of the true and the image charges. This explains the observed dependence of the droplet shape on the incident electron charge and energy, as well as on a liquid origin. Such behavior of the energies γ_{SV} and γ_{SL} should increase the contact angle for any liquids. This is in accordance with Young's equation and the developed model $\Delta\cos(\theta) \sim ((\varepsilon_S - \varepsilon_V)/(\varepsilon_S + \varepsilon_V)) - ((\varepsilon_S - \varepsilon_L)/(\varepsilon_S + \varepsilon_L))$ and the value $\Delta\cos(\theta)$ changes as Q^2, when Q is the charge density of the incident carriers. In the case of liquid, air and solid material, when ε_S and ε_L larger than $\varepsilon_V \approx 1$, square-law dewetting of the solid materials surface is observable as a result of the electron irradiation.[12]

The preliminary experimental research was conducted with various materials such as biomaterials (HAp ceramics and coatings, titanium, alumina); glass, mica and polymers; Si-based materials including p- and n-type Si, Si_3N_4, SiO_2 thin films, and Si-nanodots as well another various types of materials such as metal oxides (TiO_2, Al_2O_3).

The low-energy electron irradiation was used to achieve tunable wettability of the HAp in a wide range of contact angles.[13] The electron charging of the studied HAp samples was performed using the Kimball Physics electron gun (EFG-7, Kimball Physics Inc., USA) in vacuum 10^{-7} Torr with constant excitation energy of $E_e = 100$ eV and electron current density of $J_e = 100\ nA/cm^2$. The exposure time varied, ranging from 2 s to 1 h, in accordance to desire surface wettability state. The HAp surface properties modifications were detected by measurements of a surface electric potential and wettability variation. The XPS, XRD and AFM were used to control electrochemical, structural and topographical surface modification induced by a low-energy electron beam. The surface electric potential distribution was studied by the Kelvin probe force microscopy (KPFM). The surface hydrophobicity was studied by measuring contact angles with a sessile drop of deionized water deposited on a sample surface. The optical wettability inspection was performed by an inspection microscope (Olympus MX-50, Opelco, USA). Influence of heterogeneity (chemical or physical) of studied sample surfaces was examined by contact angle hysteresis measurements using the tilting plate technique. The volume of the liquid was kept constant (2 μl) all over the contact angle measurements of different specimens. The wettability investigations were carried out with an accuracy of $\pm 1^\circ$ at a temperature of $26 \pm 1\ ^\circ C$ and a relative humidity of $45 \pm 5\%$.

The original HAp samples demonstrate pronounced hydrophilic state with a contact angle of $\theta_0 = 10^\circ$ (Fig. 2b). The electron irradiation changes the contact angle in a very wide range from $\theta = 10^\circ$ to 100° leading to a deep wettability modulation. These measured angles appear to be stable and closely reproducible. Fig. 2 shows the variation in the water contact angles versus the incident electron charge under invariable electron beam $J_e = 100\ nA/cm^2$ and $E_e = 100$ eV. The water contact angle, θ, continuously grows with an increase of incident charge from the initial value $\theta_0 = 10$–100° with a high charge. The accuracy of the wettability tailoring may be as high as $\Delta\theta = \pm 5^\circ$ by adjusting the duration of exposure charge. Fig. 3 presents the cosine of the water contact angle as a function of the incident electron charge. The $\Delta\cos(\theta)$ increases and is proportional to the charge as Q^2, at least for a low-irradiated charge, which is consistent with developed theory of charge-induced dewetting

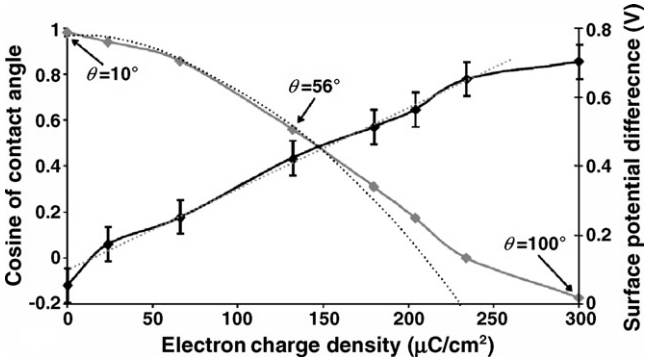

Fig. 3. Variation of the cosine contact angle of deionized water, θ (gray line), and the surface potential, $\Delta\Phi$ (black line) vs. incident electron charge density, Q. Black and gray dotted lines show the square-law and linear fitting, respectively.

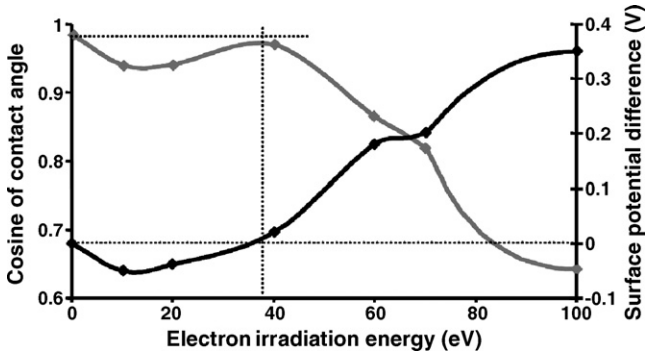

Fig. 4. Dependence of the contact angle, θ (gray line), and the surface potential, $\Delta\Phi$ (black line) vs. electron irradiation energy, E_e. The charge density is $Q = 100\,\mu C/cm^2$.

phenomena.[12] It was found that the increase of the incident electron charge up to $Q = 300\,\mu C/cm^2$ leads to saturation of cos(θ) that allows to reach $\theta = 100^\circ$ (Fig. 3). It should be noted that the increasing of the incident electron energy up to $E_e = 1$ keV results in larger penetration depth of electrons and reduction of electron-induced dewetting effect.

The measured contact angle characterizes not only the intrinsic wettability of a solid surface, but also reflects the contribution of the surface roughness and chemical heterogeneity of the observed wettability state.[14] It was found from the tilting plate measurements that hysteresis between the advancing and receding contact angles was $2 \pm 1^\circ$ for hydrophilic state ($\theta = 10^\circ$) and $14 \pm 3^\circ$ when the surface was modified to the hydrophobic state ($\theta = 100^\circ$). We attribute this hysteresis to the roughness of the HAp surfaces. Thus, the main contribution of the induced wettability may be ascribed to the variation of the surface potential.

The KFPM measurements showed that the induced average value of the surface electric potential, $\Delta\Phi$ (Fig. 3) gradually grows with the incident electron charge, Q, from $\Delta\Phi \sim 0$–0.7 V for $Q \sim 0$ and $300\,\mu C/cm^2$, respectively.

The observed flexible wettability tuning of the HAp ceramics from the initial highly hydrophilic state $\theta_0 = 10^\circ$ to a pronounced hydrophobic surface $\theta = 100^\circ$ (Fig. 2) may be unanimously ascribed to increasing trapped electron/hole charge in the vicinity of the HAp surface layer. The presented experimental data (Figs. 2 and 3) illustrates a strong influence of the injected electrons on surface electric potential of the HAp substrate. Our estimations implemented by the Monte-Carlo simulation method gave the penetration depth of the incident electrons with the used energy of $E_e = 100$ eV, around 20 Å that is consisted with the analytical method solution.[15]

In our case, the applied electron irradiation leads to electric field variation near the surface. It is created by electric charges localized at the HAp surface. The energy of primary electrons significantly exceeds the mobility gap, $E_g = 3.9$ eV, of the HAp samples, resulting in electron–hole pairs generation followed by their trapping in the vicinity of the surface and variation of the surface potential.[9,12]

The experimental data presented in Figs. 2 and 3 demonstrate the obvious correlation between the measured $\Delta\Phi$ of the HAp sample versus Q. Thus Q, which is proportional to the total number of injected electrons, allows monotonous variation of $\Delta\Phi$. The observed continuous enlargement of $\Delta\Phi$ with the absorbed charge is the evidence of the growth of the HAp band bending in $\Delta\Phi \sim 0.7$ V resulting from electron/hole filling traps (Fig. 3).

It should be noted that the observed variation of the surface potential as well as the contact angle (wettability) are fully reversible. Annealing of the preliminary electron irradiated HAp led to complete restoration of both the surface potential and wettability in the studied HAp samples. Thus, one can assume that found variation of the surface potential and wettability modulation (Figs. 2 and 3) occurs without generation or modification of bulk and surface defects. The XRD and AFM measurements of the irradiated or annealed HAp samples did not show significant changes in comparison with the untreated samples.

Dielectric charging depends on primary electron energy, E_e. The sample is negatively charged, if emission coefficient $\sigma < 1$, but it has the opposite charge if $\sigma > 1$. There is a specific value of the primary electrons' energy, E_e^*, at which $\sigma = 1$. The value of E_e^* in HAp is unknown. However, for most of the dielectric materials the value of E_e^* is several dozens of eV.[16,17] Fig. 4 illustrates the experimental verification, which shows a dependence of the cosine of the water contact angle and the surface potential on E_e, ranging from 0 to 100 eV, when Q was constant for all varieties of energies ($Q = 100\,\mu C/cm^2$). A minimal dewetting effect is observed when the energy $E_e \sim 40$ eV and $\Delta\Phi$ close to E_e passes through zero.

Investigation of the HAp sample retention, after applying the wettability patterning, shows that tailored hydrophilic and hydrophobic states stay stable at least during the month in different environment conditions, such as air and water.

5. Biocells immobilization on modified hydroxyapatite surface

Surface energy modification of biological substrates provides optimal conditions for biocells adhesion following by their growth and proliferation. Numerous experimental data show that biocells of different origin demonstrate dissimilar affinity to modified bio-substrates. The proposed and widely used surface modification techniques modulate the surface energy in controllable but strictly definite on/off mode.[1–4]

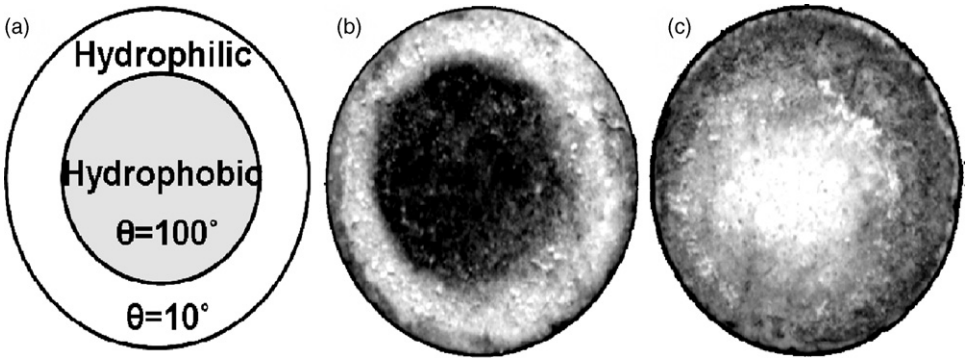

Fig. 5. (a) Schematic illustration of hydroxyapatite patterned surface (θ is the contact angle). (b) Adhesion of BSA and (c) DNA to the hydroxyapatite surfaces with different wettability state.

In the case of the developed charge-induced wettability engineering method,[5,7,13] tailoring of any wettability state occurs in a large range of contact angles, $\Delta\theta \sim 100^\circ$ with high accuracy reaching $\pm 5^\circ$ by controlling the number of incident and trapped electron/hole charges (Figs. 2–4).

Biological cells with different basic properties such as biomolecules bovine serum albumin proteins (BSA) and deoxyribonucleic acid (DNA) as well as Gram-negative *Escherichia coli* (*E. coli*) and *Pseudomonas putida* (*P. putida*), and Gram-positive *Bacillus subtilis* (*B. subtilis*) bacteria were used to study the influence of wettability modification of the treated HAp surface on biocells immobilization. The chosen BSA and DNA molecules have opposite wettability affinity to a substrate. Experimental evidences suggest that the hydrophobic interaction is the major determinant of protein adsorption, whereas DNA prefers the more hydrophilic substrates.[6,18] The susceptibility of biomaterials to bacterial adhesion is determined by several factors, such as chemical composition of the surface, fine topography roughness, surface electric charge as well wettability state.[19]

BSA and single stranded salmon sperm DNA (Sigma–Aldrich Corporation, St. Louis, MO, USA) were dissolved in distilled water at a concentration of 1 mg/ml and applied to the treated HAp ceramic surface (the volume of the solution was 100 ml). Since the DNA and BSA concentration was quiet low the pH was that of the water (~5.5). The samples were incubated 15 min. at room temperature with no vibrations, washed several times with distilled water and then stained with 0.05% Toluidine blue (in ethanol) to visualize the biomolecules.

Bacteria used were grown in LB medium (Difco, sparks, MD, USA) at 37 °C with vigorous agitation to stationary growth phase. The bacteria were applied on the HAp ceramics surface and incubated at room temperature for 20 min. The HAp surface was washed with 150 mM NaCl and stained with 0.05% Toluidine blue (in ethanol).

Two sets of HAp samples with wettability modified surfaces were fabricated. In the first set series of the HAp ceramics samples were subjected to electron irradiation using increasing exposition time intervals, resulting in fabrication of several specimen-substrates with various wettability states. The second set of the HAp substrates included wettability patterned samples where the irradiation of the HAp substrate was performed via specific mask to fabricate highly hydrophobic center, whilst the sample periphery remained hydrophilic (Fig. 5a).

The results on adhesion of BSA and DNA on the patterned HAp ceramic substrate show dramatic difference in affinity of these biomolecules to the tailored wettability state. BSA was immobilized in the central hydrophobic part of the substrate only (Fig. 5b) whereas DNA molecules were adhered at the peripheral hydrophilic region of the patterned HAp (Fig. 5c). Such a differential binding of BSA and DNA is consistent with studied wettability properties of these molecules.[6,18] DNA is very hydrophilic molecules due to the phosphate groups in the sugar-phosphate backbone, bound preferentially to the high wettability surface. In contrast, the binding of BSA, a protein which contains hydrophobic domains is more pronounced at low wettability.

Another set of the HAp samples with gradually varied tailored wettability state ranging from $\theta = 10$–100° with a step of $\Delta\theta \sim 10^\circ$ was targeted by three different sorts of bacteria Gram-negative *E. coli*, Gram-positive *B. subtilis* and Gram-negative *P. putida*. The full results of immobilization on the fabricated HAp samples are presented in Fig. 6. The experimental results on adhesion of the bacteria showed that the

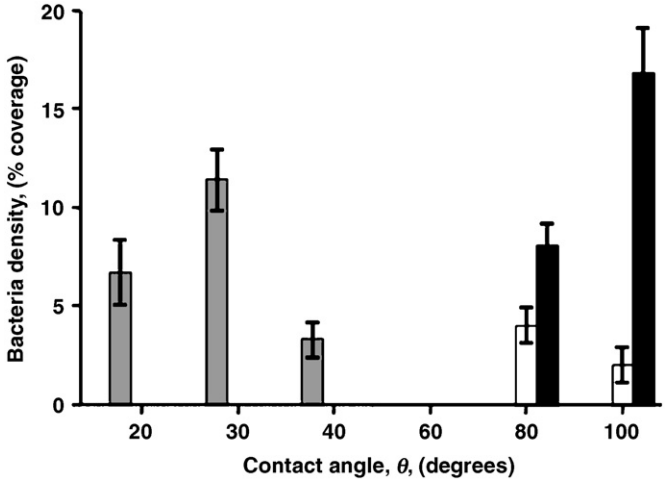

Fig. 6. Adhesion of various bacteria (gray, white and black bars refer to *E. coli*, *P. putida*, and *B. subtilis*, respectively) on the hydroxyapatite surface as a function of wettability modulation. The proportion of the total field of view that is covered by settled bacteria is determined by image analysis and is expressed as percentage coverage. The error bars refer to the statistical errors.

distribution of the *E. coli* adhesion is distinctly selective on the HAp surface around a contact angle of $\theta \sim 30^\circ$. Adhesion of the *B. subtilis* is observed at the hydrophobic HAp substrate state starting from the contact angle of $\theta \sim 80^\circ$ and increased its adhesive affinity with the increasing of the contact angle up to $\theta \sim 100^\circ$. The *P. putida* bacteria demonstrate another behavior. Its adhesion shows a maximum for $\theta \sim 80^\circ$ and then gradually reduces with the increasing of the HAp substrate hydrophobicity. The selective adhesion may be related to different bacterial hydrophobicity, since bacteria adhere differently to materials with different wettability state depending on the hydrophobicity of both bacteria and material surface.[19]

Thus the developed methods allows fabricating different susceptibilities of biomaterials surface to infections, because adhesion and growth of infecting bacteria may be controlled by the HAp surface properties, like hydrophobicity.

6. Conclusions

Studies of physical properties of the HAp bioceramics performed in this work showed that it may be related to a wide band gap semiconductor with numerous electron/hole traps.

The developed low-energy electron irradiation method leads to pronounced tunable variation of the HAp ceramics' and coatings' wettability state which is considered as a basic mechanism responsible for the biocells–substrate integration. The main advantages of the method are as follows: (i) imprinting of the modified wettability with high resolution, (ii) tailoring and tuning of the wettability state in a wide range (contact angles ranging from 10° to 100°), and (iii) fabricating micro/nano patterned bio-templates.

It is shown that found method of the HAp wettability modification allows tailoring and patterning of specific hydrophobic/hydrophilic states needed for selective adhesion/non-adhesion of basic biomolecules and bacteria on the HAp biosubstrates. Thus the developed method allows fabricating different susceptibilities of biomaterials to proteins and DNA biomolecules adhesion. On the other hand the method may be used to change the surface affinity to infections, because adhesion and growth of infecting bacteria may be controlled by the HAp surface properties, like hydrophobicity.

Acknowledgements

The authors are thankful to Prof. G. Mezinskas (Institute of Silicate Materials, Riga Technical University, Riga, Latvia) for the HAp ceramics fabrication, and Prof. E.Z. Ron (Tel-Aviv University, Israel) for support in biological part of experiments. This research was supported by the European commission project NMP3-CT-504937 "PERCERAMICS".

References

1. Lahann, J. and Langer, R., Smart materials with dynamically controllable surfaces. *MRS Bull.*, 2005, **30**, 185–188.
2. McCaig, C. D. and Zhao, M., Physiological electrical fields modify cell behaviour. *BioEssays*, 1997, **19**, 819–826.
3. Jelinski, L., In *Nanostructure Science and Technology*, ed. R. W. Siegel, E. Hu and M. C. Roco. Kluwer Academic Publishers, Dordrecht, The Netherlands, 1999 [chapter 7].
4. Clark, W. B., Lane, M. D., Beem, J. E., Bragg, S. L. and Wheeler, T. T., Relative hydrophobicities of *Actinomyces viscosus* and *Actinomyces naeslundii* strains and their adsorption to saliva-treated hydroxyapatite. *Infect. Immun.*, 1985, **47**, 730–736.
5. Rosenman, G., Aronov, D. and Dekhtyar, Yu., Method and device for wettability modification of materials. US Patent Application No. 60/730 021 Pending.
6. Wilson, C. J., Clegg, R. E., Leavesley, D. I. and Pearcy, M. J., Mediation of biomaterial–cell interactions by adsorbed proteins. A review. *Tissue Eng.*, 2005, **11**, 1–18.
7. Aronov, D., Rosen, R., Ron, E. Z. and Rosenman, G., Tunable hydroxyapatite wettability: effect on adhesion of biological molecules. *Proc. Biochem.*, 2006, **41**, 2367–2372.
8. Posner, A. S., Crystal chemistry of bone mineral. *Physiol. Rev.*, 1969, **49**, 760–792.
9. Rosenman, G., Aronov, D., Oster, L., Haddad, J., Mezinskis, G., Pavlovska, I. *et al.*, Photoluminescence and surface photovoltage spectroscopy studies of hydroxyapatite nano-bio-ceramics. *J. Lumin.*, 2007, **122-123**, 936–938.
10. Young, T., An essay on the cohesion of fluids. *Philos. Trans. R. Soc. Lond.*, 1805, **95**, 65–87.
11. Lippmann, G., Relation entre les phenomenes electriques et capillaries. *Ann. Chim. Phys.*, 1875, **5**, 494–549.
12. Aronov, D., Molotskii, M. and Rosenman, G., Charge-induced wettability modification. *Appl. Phys. Lett.*, 2007, **90**., doi:10.1063/1.2711656.
13. Aronov, D., Rosenman, G., Karlov, A. and Shashkin, A., Wettability patterning of hydroxyapatite nanobioceramics induced by surface potential modification. *Appl. Phys. Lett.*, 2006, **88**, 163902–163904.
14. Joanny, J. F. and de Gennes, P. G., A model for contact angle hysteresis. *J. Chem. Phys.*, 1984, **81**, 552–562.
15. Morbitzer, L. and Scharmann, A., Messung der eindringtiefe von elektronen und ionen in dünnen aufdampfschichten. *Z. Phys.*, 1964, **181**, 67–86.
16. Schreiber, E. and Fitting, H.-J., Monte Carlo simulation of secondary electron emission from the insulator SiO_2. *J. Electron Spectrosc. Relat. Phenom.*, 2002, **124**, 25–37.
17. Hatfield, L. L. and Adamson, E. R., The low energy crossover point for secondary electron emission fromLexan. IEEE 1994 Annual Report. Conference on Electrical Insulation and Dielectric Phenomena, 1994, pp. 256–261.
18. Tilton, R. D., Robertson, C. R. and Gast, A. P., Manipulation of hydrophobic interactions in protein adsorption. *Langmuir*, 1991, **7**, 2710–2718.
19. An, Y. H. and Friedman, R. J., Concise review of mechanisms of bacterial adhesion to biomaterial surfaces. *J. Biomed. Res.*, 1998, **43**, 338–348.